Springer

Journal of
Mechanical
Science and
Technology

Journal of Mechanical Science and Technology 22 (2008) 497~505

www.springerlink.com/content/1738-494x

Fuzzy MRAC controller design for vane-type air motor systems

Yean-Ren Hwang[1,*], Yu-Da Shen[2] and Kuo-Kuang Jen[2]

[1]*Professor, Department of Mechanical Engineering and the Institute of Opto-Mechatronics Engineering, National Central University, Chung-Li, Taiwan 320.*

[2]*Ph.D. student, Department of Mechanical Engineering, National Central University, Chung-Li, Taiwan 320.*

(Manuscript Received May 18, 2007; Revised December 14, 2007; Accepted December 14, 2007)

Abstract

Air motors are widely used in the automation industry due to special requirements, such as spark-prohibited environments, the mining industry, chemical manufacturing plants, and so on. The purpose of this paper is to analyze the behavior of a vane-type air motor and to design a model reference adaptive control (MRAC) with a fuzzy friction compensation controller. It has been noted that the rotational speed of the air motor is closely related to the compressed air's pressure and flow rate, and due to the compressibility of air and the friction in the mechanism, the overall system is actually nonlinear with dead-zone behavior. The performance of the previous controllers implemented on an air motor system demonstrated a large overshoot, slow response and significant fluctuation errors around the setting points. It is important to eliminate the dead-zone to improve the control performance. By considering the effects of the dead-zone behavior, we have developed an MRAC with fuzzy friction compensation controller to overcome the effect of the dead-zone. The following experimental results are given to validate the proposed speed control strategy.

Keywords: Air motor; Dead-zone; MRAC; Fuzzy logic controller

1. Introduction

Modern automation techniques have been helping manufacturers to improve the quality of products and reduce the cost of the manufacturing process. Although electrical motors are still the main conveying devices in most manufacturing plants, air motors have attracted more and more attention during the past few decades because they are cheaper, safer, cleaner, smoother and more efficient (by maintaining a higher power to weight ratio) [1-4]. Moreover, at some special locations, such as spark-prohibited environments, the mining industry, chemical manufacturing plants, vehicles and/or storage facilities with explosive materials, etc., the air motor will be more efficient and sometimes may be the only device that can be used.

Air motors convert the energy of compressed air into mechanical energy. In general, air motors demonstrate highly nonlinear behavior due to the compressibility of air and the friction of the mechanisms. In the speed control system, the air motor shows a variable dead-zone in the control input for different frequency of applied input signals. Hence, it is difficult to design a speed controller which realizes accurate speed control at any time. Up to now, there have been several investigations and analyses on the dynamics of air motors in previous articles. The proportional integral (PI) controller was proposed in [2]; the all air motor system was considered as a first order linear system. Although the PI control algorithm is simple and has high-reliability when the PI values are adjusted very well, the PI controller cannot retain the performance all the time because the air motor has nonlinear speed characteristics under different operating conditions. In [5], a nonlinear system was developed by considering all nonlinear phenomena such as unmodeled uncertainties. However, these uncertain

*Corresponding author. Tel.: +886 3 4267342 Fax.: +886 3 4254501
E-mail address: yhwang@cc.ncu.edu.tw
DOI 10.1007/s12206-007-1204-5

factors actually affected the performance of pneumatic devices and the air motor, and hence it may be better to analyze these nonlinear phenomena. A fourth-order nonlinear model was developed in [6] and its parameters were identified through experiment data. However, due to its complexity, this model has a large number of parameters; thus the process of deriving parameters is complicated and time consuming. A different approach using neural network techniques is proposed in [7]. Instead of developing a high order nonlinear model, a neural-model reference control by adopting neural network techniques was proposed to control the rotational speed of the air motor. The air motor described in previous articles was mostly operated at low speed range. The control algorithms for air motor have a very large overtime, long rise time and cannot compensate for the effect of a dead-zone [2, 3, 7].

Air motors have uncertain speed characteristics. In most practical motion systems, the dead-zone parameters are poorly known [8]. The dead-zone is a problem as an accurate speed actuator for industrial applications, and how to eliminate it in order to improve the control performance is very important. Air motors demonstrate a variable dead-zone when the control input signals are different. Hence, it is difficult to design a speed controller which achieves accurate speed control at all times and takes into account the system dynamic response deterioration due to the dead-zone. To overcome the dead-zone problem, a speed control scheme for the air motor with dead zone compensation is investigated in this paper. In the proposed control scheme, a MRAC with fuzzy friction compensation of the dead-zone was implemented to determine the dead-zone compensation input and improve the performance of the system [9,10]. The MRAC was applied to an air motor with unknown parameters and friction [11]. The MRAC retains the system output of tracking the reference model and provides robust performance against the unknown parameter variation [9].

The fuzzy logic control has been discussed in many articles for nonlinear systems [12-14] but few have dealt with the applications for having a dead-zone phenomenon such as air motors. Basically, a fuzzy logic controller contains three major processes [12,14]: fuzzification, fuzzy inference and defuzzification. In the fuzzification process, physical measurements will be transformed to fuzzy variables, which are described by fuzzy sets [15]. The rules used in the fuzzy inference process are usually created according to experts' experience and knowledge [12-14]. The control results as fuzzy variables will be induced through fuzzy set operations based on these rules. In the defuzzification process, these results will be used to calculate the physical control inputs, such as voltages, currents, and so on. Further, we will apply the fuzzy control algorithms to overcome the dead-zone phenomenon and obtain faster, non-overshooting and less chattering response for air motor control.

The following sections are organized as follows: the introduction to a vane type air motor system is described in Section 2, the nonlinear behavior of the air motor system is analyzed in Section 3, the MRAC algorithm is designed in Section 4, the dead-zone compensation using fuzzy inference is proposed in Section 5, the experimental results are shown in Section 6 and the conclusion is stated in Section 7.

2. Vane type air motor system

Fig. 1 shows the sketched map of a vane-type air motor. There is a rotational drive shaft with four slots, each of which is fitted with a freely sliding rectangular vane. When the drive shaft starts to rotate, the vanes tend to slide outward due to centrifugal force and are limited by the shape of the rotor housing. Depending on the flow direction, this motor will rotate in either a clockwise or counterclockwise direction. The difference in air pressure at the inlet and outlet will provide the torque required to move the shaft. Hence, the higher flow rate and the larger pressure difference will provide a larger torque on the shaft and higher rotational speed.

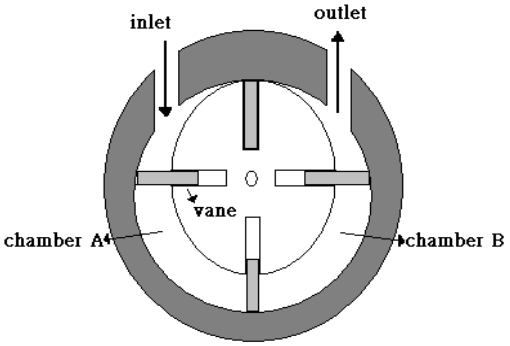

Fig. 1. Vane-type air motor.

The air motor system, as shown in Fig. 2(a), consists of an air motor (GAST 1AM), an air tank, an electronic proportional directional control valve (FESTO MPVE), a filter/regulator with lubricant (SHAKO FRL-600) and a digital signal processor (DSP, TI C240). The airflow path starts from the air tank through the filter, control valve and finally enters the air motor. The airflow entry in the motor will be determined by the valve position, which is controlled by externally applied voltage, denoted by v. When v equals 5V, the valve will stay at the middle and both left and right entries will be closed. The valve will move right when v is above 5V and fully opened when v is equal to 10V. Similarly, the valve will move left if v is less than 5V, and will be fully opened at 0V. The direction of the air motor depends on whether the voltage v is above or below 5V. The control input from DSP, denoted by u, will be converted into v as $v=u+5$. The experimental air motor system is shown in Fig. 2(b).

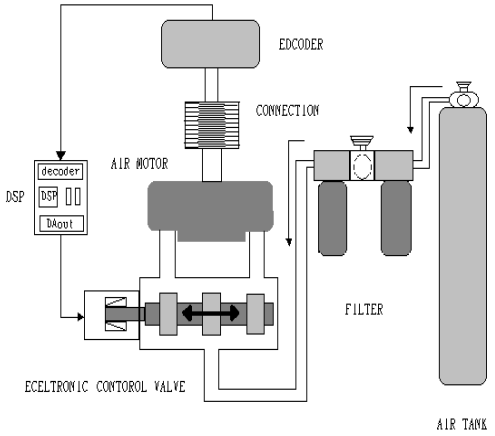

Fig. 2(a). The schematic diagram of the air motor system.

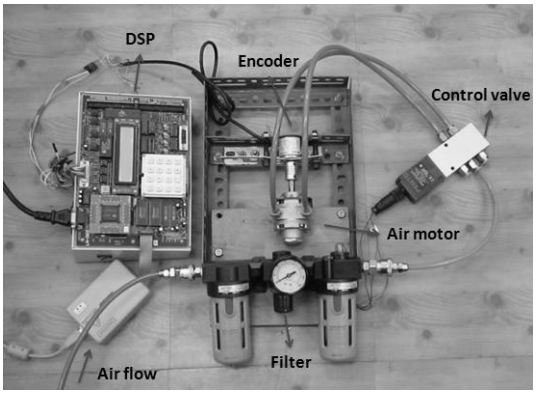

Fig. 2(b). The experimental air motor system.

3. Nonlinear behavior of air motor system

Fig. 3(a), (b), (c) show the results of the experiments we designed for researching the relationship

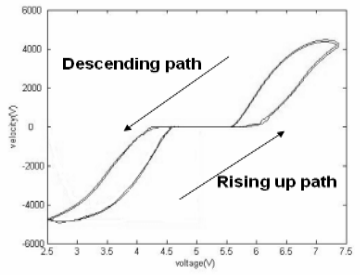

(a)

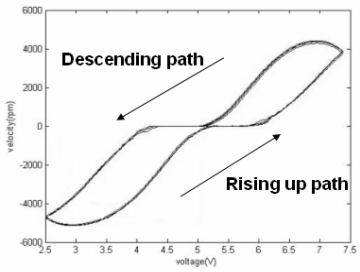

(b)

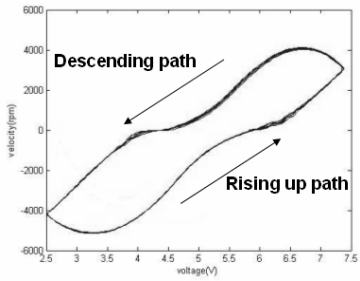

(c)

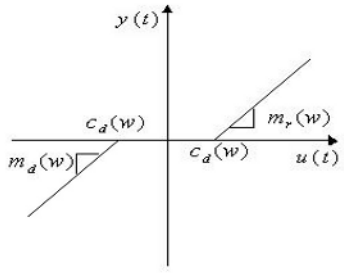

(d)

Fig. 3. The static relationship between the applied voltage and rotational speed (the input frequencies in (a), (b), (c) are 0.2 Hz,0.4 Hz and 0.8 Hz, respectively. (d) is dead-zone model).

between the applied input voltage and the rotational speed of the air motor. During the experiment, *u* was adjusted following the cycle 0V→ 2.5V→ -2.5V→ 0V at different frequencies. The input frequencies in Fig. 3(a), (b) and (c) are 0.2Hz, 0.4Hz and 0.8Hz, respectively. It was found that there existed a dead-zone phenomenon for this system. The voltage-speed curve demonstrated different relationships during the voltage increasing and decreasing procedures. For example, in Fig. 3(a) with the input frequency as 0.2Hz, the motor remained motionless when the voltage was less than 1V during the increasing procedure. However, after exceeding 1V, the voltage and rotational speed demonstrated a linear relationship. When the voltage was reduced from 2.5V to 0V, the speed-voltage relationship did not follow the same path of rising up but demonstrated nonlinear behavior. Also, the motor stopped around 0.8V instead of 1V. Similar results were found for the procedures when the voltage was below 0V.

As shown in Fig. 3(a), (b), (c), the dead-zone varies for different input frequency w. Hence, the dead-zone with input *u(t)* and output *y(t)* can be described by:

$$y(t)=\begin{cases} m_r(w)(u(t)-c_r(w)) & if \quad u(t)\geq c_r(w) \\ 0 & if \quad c_d(w)<u(t)<c_r(w) \\ m_d(w)(u(t)-c_d(w)) & if \quad u(t)\leq c_d(w) \end{cases} \tag{1}$$

where the parameters $m_r(w)$, $m_d(w)$, $c_r(w)$, $c_d(w)$, as shown in Fig. 3(d), are the rising slope, the decreasing slope, the rising path offset voltage and the decreasing path offset voltage, respectively. These parameters are bounded but depend on the frequency of the motions.

4. Model reference adaptive controller design

First, the system was considered as following an *n*th order differential equation

$$y^n+\alpha_{n-1}y^{n-1}+\cdots+\alpha_1\dot{y}+\alpha_0 y=\beta(u-f) \tag{2}$$

where *y* is an output variable, *u* is a control variable, *f* is an unknown friction(dead zone) and bounded, a_i (i=0,1,2,3,…n-1) and β >0 are unknown constant parameters.

The model reference is described as

$$y_m^n+\omega_{n-1}y_m^{n-1}+\cdots+\omega_1\dot{y}_m+\omega_0 y_m=\beta_m u_m \tag{3}$$

where y_m is reference output, u_m is a command input. The tracking error is defined as $e=y_m-y$, then the error equation is

$$\begin{aligned} &e^n+\omega_{n-1}e^{n-1}+\cdots+\omega_1\dot{e}+\omega_0 e= \\ &\beta_m u_m-\beta u+\beta f+\sum_{i=0}^{n-1}(\alpha_i-\omega_i)y^i \end{aligned} \tag{4}$$

We assume that $\beta=\beta_0+\Delta\beta$, β_0 is the nominal value. The control *u* is designed as

$$u=\frac{\beta_m u_m}{\beta_0}+kx+u_{ad}+u_f \tag{5}$$

where $k=\left[k_0k_1\cdots k_{n-1}\right]^T$ is feedback gain matrix, $x=\left[e_0e_1\cdots e_{n-1}\right]^T$ is system state vector, u_{ad} is adaptive law and the u_f is a control input for friction compensation. The eq(4) can be written as

$$\begin{aligned} &e^n+\omega_{n-1}e^{n-1}+\cdots+\omega_1\dot{e}+\omega_0 e \\ &=-\beta_0 kx-\beta u_{ad}-\frac{\Delta\beta}{\beta_0}\beta_m u_m-\Delta\beta kx \\ &\quad -\beta u_f+\beta f+\sum_{i=0}^{n-1}(\alpha_i-\omega_i)y^i \end{aligned} \tag{6}$$

The above equation can be changed to a canonical state-space form

$$\dot{x}=Fx-G\beta u_{ad}+G\sigma^T\varphi+G\beta(f-u_f) \tag{7}$$

where

$$F=\begin{bmatrix} 0 & 1 & \cdots & 0 \\ \cdot & \cdot & \cdot & \cdot \\ 0 & \cdot & \cdot & 1 \\ -\omega_0-\beta_0k_0 & \cdot & \cdot & -\lambda\omega_{n-1}-\beta_0k_{n-1} \end{bmatrix}$$

$$G=\begin{bmatrix} 0 \\ \cdot \\ \cdot \\ \cdot \\ 1 \end{bmatrix}$$

$$\sigma=\left[u_m \quad kx \quad y \quad \cdots \quad y^{n-1}\right]^T,$$

$$\varphi=\left[\frac{-\Delta\beta\beta_m}{\beta_0} \quad -\Delta\beta \quad \alpha_0-\omega_0 \quad \cdots \quad \alpha_{n-1}-\omega_{n-1}\right]^T$$

The k we choose can let the F matrix be a Hurwitz matrix. For a globally asymptotical stable system, a positive definite matrix Q is to be chosen such that there exists a symmetric positive matrix P satisfying

$$F^TP+PF=-Q \tag{8}$$

According to the Eq(7), we defined $\phi=1/\beta$

$$u_{ad} = \hat{\phi}\,\sigma^T\hat{\varphi} \tag{9}$$

$$\dot{\hat{\varphi}} = \gamma\sigma Cx, \qquad \gamma = const > 0 \tag{10}$$

$$\dot{\hat{\phi}} = \gamma_1 x^T C^T \sigma^T \hat{\varphi}, \qquad \gamma_1 = const > 0 \tag{11}$$

$$C = G^T P \tag{12}$$

where $\dot{\hat{\varphi}}$ and $\dot{\hat{\phi}}$ are the adaptive estimate of the constant vector φ and the constant $\phi=1/\beta$.

Defining the adaptive estimate errors as

$$\tilde{\varphi} = \hat{\varphi} - \varphi \;;\; \tilde{\phi} = \hat{\phi} - \phi \tag{13}$$

and then we also can obtain

$$\dot{\tilde{\varphi}} = \gamma\sigma Cx \tag{14}$$

$$\dot{\tilde{\phi}} = \gamma_1 x^T C^T \sigma^T \hat{\varphi} \tag{15}$$

Substituting Eq(13) into the Eq(7), the system can be written as

$$\dot{x} = Fx - G\beta\tilde{\phi}\sigma^T\hat{\varphi} - G\sigma^T\tilde{\varphi} - G\beta u_f + Gbf \tag{16}$$

The Lyapunov function is

$$V = x^TPx + \frac{1}{\gamma}\tilde{\varphi}^T\tilde{\varphi} + \frac{\beta}{\gamma_1}\tilde{\phi}^2 \tag{17}$$

The derivative of V can be evaluated as

$$\begin{aligned}\dot{V} &= x^T(F^TP + PF)x - 2x^TPG\sigma^T\tilde{\varphi} \\ &\quad - 2x^TPG\beta\tilde{\phi}\sigma^T\hat{\varphi} + \frac{2}{\gamma}\tilde{\varphi}^T\dot{\tilde{\varphi}} + \frac{2\beta}{\gamma_1}\tilde{\phi}\dot{\tilde{\phi}} \\ &\quad + 2x^TPG\beta\left[f - u_f\right] \\ &= - x^TQx - 2x^TPG\sigma^T\tilde{\varphi} + 2\tilde{\varphi}^T\sigma Cx \\ &\quad - 2x^TPG\beta\tilde{\phi}\sigma^T\hat{\varphi} + 2\beta\tilde{\phi}x^TC^T\sigma^T\tilde{\varphi} \\ &\quad + 2x^TC^T\beta\left[f - u_f\right] \\ &= - x^TQx + 2x^TC^T\beta\left[f - u_f\right]\end{aligned} \tag{18}$$

If the $u_f = K_s\,\mathrm{sgn}(Cx)$ and $K_s = \sup(|f|)$, then the $\dot{V} = -x^TQx \le 0$. The system will approach zero asymptotically. The whole control scheme can be summarized as follows：

$$u = \frac{\beta_m u_m}{\beta_0} + kx + \hat{\phi}\sigma^T\hat{\varphi} + K_s\,\mathrm{sgn}(Cx) \tag{19}$$

$$\dot{\hat{\varphi}} = \gamma\sigma Cx, \qquad \gamma = const > 0$$

$$\dot{\hat{\phi}} = \gamma_1 x^T C^T \sigma^T \hat{\varphi}, \qquad \gamma_1 = const > 0$$

$$C = G^TP$$

$$\sigma = \left[u_m \quad kx \quad y \quad \cdots \quad y^{n-1}\right]^T$$

It is noted from the experimental results that the bandwidth of the electric control valve is much larger than that of air motors [2], and the controller is designed to control the speed of air motors in this paper. Therefore, we considered the air motor system and reference model system as a first order system. For comparison purposes, the reference signal is a sinusoidal wave with the frequency of 0.1 Hz, 0.25 Hz and 0.5 Hz and the notations y_m and y represent the reference signal and experimental results in the following Figs, respectively.

The presence of a dead-zone in a mechanical system is often responsible for the system characteristics. The dead-zone changes with time and with environmental factors. The straightforward solution is that the control input adds a value, like $u_f = K_s\,\mathrm{sgn}(Cx)$ and $K_s = \sup(|f|)$, to eliminate dead-zones. The frequency of the referential sinusoidal wave is 0.5 Hz, and the result of speed control of MRAC without friction compensation is shown in Fig. 4. The system output could not track the reference signal well. There is a terrible tracking error when the proposed controller does not compensate for friction. It can be seen at Fig. 5, the proposed controller with $u_f = K_s\,\mathrm{sgn}(Cx)$, Ks is arbitrarily constant value and $K_s > \sup(|f|)$, compensation seems to overcome the influence of a dead-zone when the frequency of referential sinusoidal wave is 0.5 Hz. However, in Figs. 6 and 7 the experimental results of the air motor with

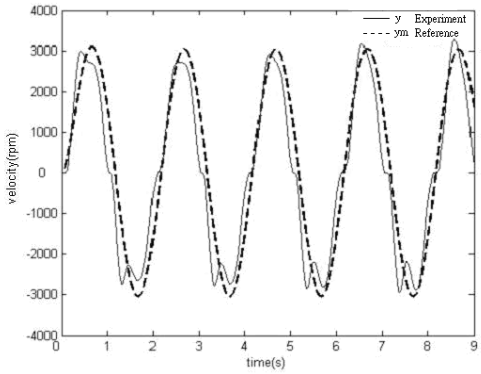

Fig. 4. MRAC without friction compensation.

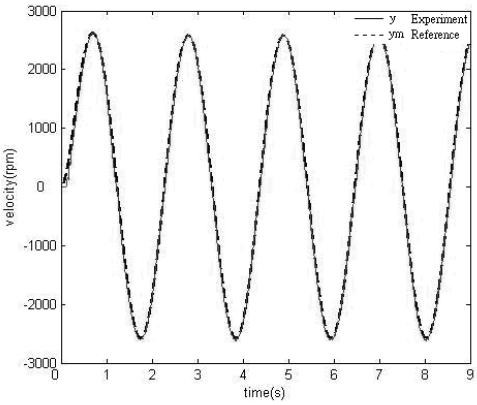

Fig. 5. MRAC with friction compensation.

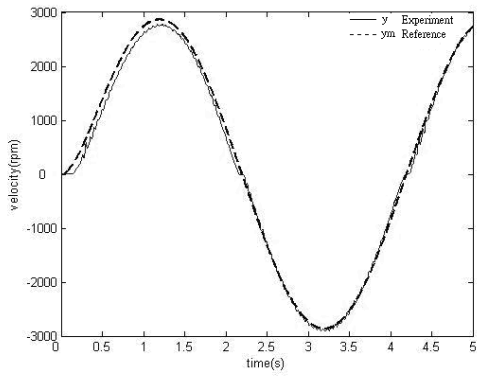

Fig. 6. MRAC with friction compensation, $u_f = K_s \operatorname{sgn}(Cx)$,K_s is too small to eliminate dead-zone (the frequency of referential sinusoidal wave is 0.25 Hz).

$u_f = K_s \operatorname{sgn}(Cx)$ have a large tracking error at low speed (or at dead-zone) when the frequency of the referential sinusoidal waves is 0.25 Hz and 0.1 Hz, respectively. It appears as though the value *Ks* is too small to eliminate the dead-zone, so that if the value *Ks* is large enough, the tracking error will decrease at low speed. Figs. 8-9 show that when the value *Ks* is large enough to overcome the effect of a dead-zone, the frequency of referential sinusoidal wave is 0.25 Hz and 0.1 Hz, respectively. But the whole system has severe chattering phenomenon. According to the above experimental results, if we want to have good control performance, the constant value *Ks* is not suitable for whole reference signals, because the dead zone varies from difference reference signals.

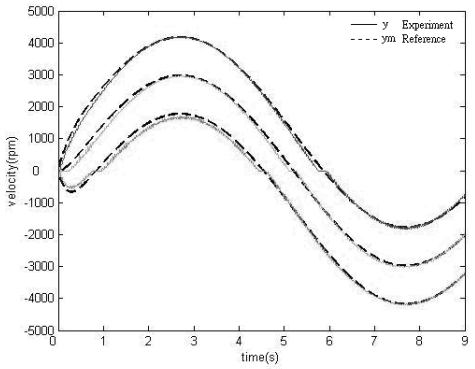

Fig. 7. MRAC without friction compensation, $u_f = K_s \operatorname{sgn}(Cx)$, K_s is too small to eliminate dead-zone (the frequency of referential sinusoidal wave is 0.1 Hz).

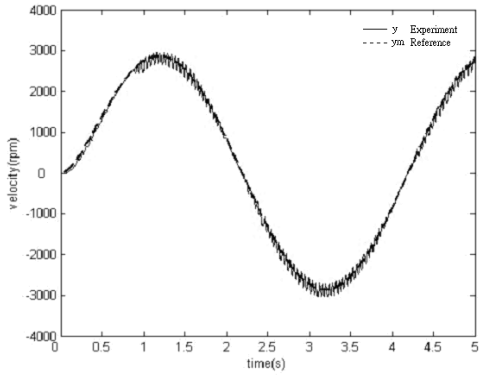

Fig. 8. MRAC with friction compensation, $u_f = K_s \operatorname{sgn}(Cx)$, K_s is enough to eliminate dead-zone (the frequency of referential sinusoidal wave is 0.25 Hz).

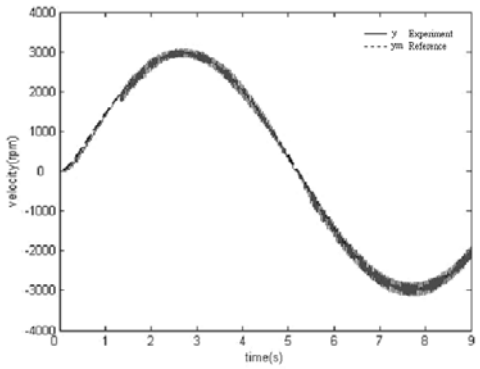

Fig. 9. MRAC with friction compensation, $u_f = K_s \operatorname{sgn}(Cx)$, K_s is enough to eliminate dead-zone (the frequency of referential sinusoidal wave is 0.1 Hz).

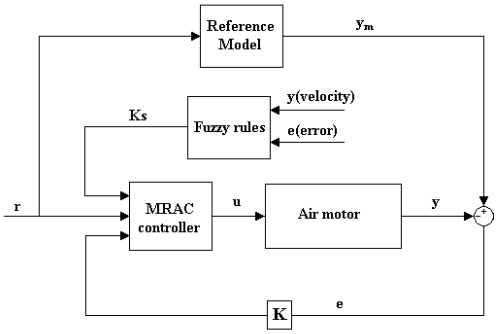

Fig. 10. Block diagram of speed control using dead-zone compensation with fuzzy rules and MRAC controller.

5. Dead-zone compensation using fuzzy inference

For MRAC controller, if the *Ks* is too large, it will cause a heavy chattering phenomenon. If the *Ks* is too small, the speed tracking error will increase at low speed. The dead-zone width of an air motor varies from different reference signals. Therefore, the best scheme is that the value *Ks* can be adjusted with the time so that the air motor system does not have heavy chattering phenomenon and the tracking error can decrease as time goes by. In order to achieve this goal, we use fuzzy control to adjust the value *Ks* to the current control environment.

The fuzzy rules for dead-zone compensation are shown in Table 1. Fig. 10 shows a block diagram of speed control using dead-zone compensation with fuzzy rules and MRAC controller. The fuzzy rules for dead-zone compensation, which include the speed tracking error *e* and the experiment speed *y* in the speed control, are designed as

Table. 1. Rule matrix for fuzzy dead-zone compensation.

Rule matrix for fuzzy dead-zone compensation

Δu_f	Velocity V						
Error E	*NB*	*NM*	*NS*	*Z*	*PS*	*PM*	*PB*
NB	*NB*	*NB*	*NB*	*NB*	*NM*	*NS*	*NS*
NM	*NM*	*NM*	*NM*	*NM*	*NS*	*NS*	*Z*
NS	*NS*	*NS*	*NS*	*NS*	*NS*	*Z*	*PS*
Z	*NS*	*NS*	*Z*	*Z*	*Z*	*PS*	*PS*
PS	*NS*	*Z*	*PS*	*PS*	*PS*	*PS*	*PS*
PM	*Z*	*PS*	*PS*	*PM*	*PM*	*PM*	*PM*
PB	*PS*	*PS*	*PM*	*PB*	*PB*	*PB*	*PB*

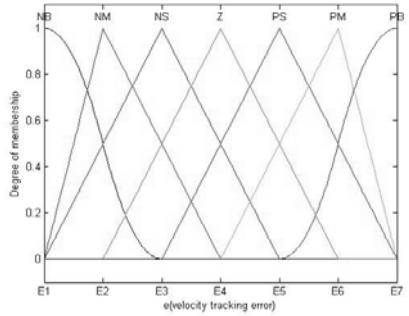

(a)

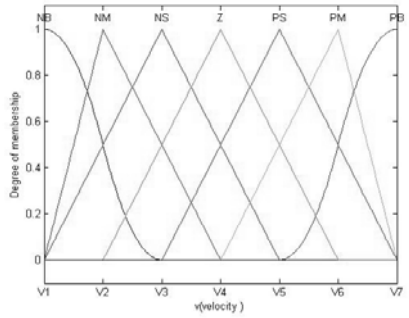

(b)

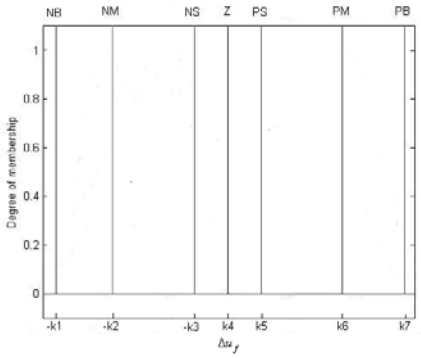

(c)

Fig. 11. The membership of error[Fig. 11(a)], speed[Fig. 11(b)] and Δu_f [Fig. 11(c)].

Rule *i*: if e is E_j and y is V_x then Δu_f is K_g

i=1,2,3…….48,49 ; *j*=1,2,..7 ; *x*=1,2,..7 ;

g=1,2,..7 ;

The membership functions of E_j, V_x, and K_g are shown in Fig. 11. The notations in these figures, NB, NM, NS, Z,PS, PM, PB, etc., represent the fuzzy sets; for instance, NB represents "negative big," PS represents "positive small," and so on.

Defuzzification is the process of converting a fuzzy quantity, represented by a membership function, to a crisp value. The weighted average method, defining the crisp value as the weighted average of membership functions, is a commonly used in industry. This method is valid only for the case where the output membership function is a union result of several fuzzy quantities [15].

$$\Delta u_f = \sum_{i=1}^{49} w_i K_g \Big/ \sum_{i=1}^{49} w_i \tag{20}$$

where w_i represent the weighted value of that membership function.

The control input of compensation for friction u_f is described as

$$\begin{aligned} K_s(k) &= K_s(k-1) + \Delta u_f(k) \\ u_f(k) &= K_s(k) \cdot \mathrm{sgn}(Cx) \end{aligned} \tag{21}$$

6. Experimental results

The proposed fuzzy rules were described earlier, and the experimental results of the speed control of MRAC with fuzzy friction $u_f = K_s \,\mathrm{sgn}(Cx)$ compensation are shown in Figs. 12 and 13. We find that the fuzzy control retains good performance and eliminates the effect of dead zone of the air motor.

According to the experimental results, there is a serious performance result without fuzzy algorithm in the dead-zone region when the frequency of the reference sinusoidal signal is slow. The tracking error is about 10%. If the K_s from MRAC with friction compensation ($u_f = K_s \,\mathrm{sgn}(Cx)$) is enough to eliminate a dead-zone caused by friction, it is successful in eliminating the dead-zone problem but the system has chattering with tracking error 15% phenome non. With K_s from MRAC with fuzzy friction ($u_f = K_s \,\mathrm{sgn}(Cx)$) compensation, the fuzzy rules can modulate an adequate compensative value to overcome the chattering and dead-zone problem. Finally, the results from Figs. 12-13 show that the method, fuzzy MRAC with friction compensation, proposed for this system eliminated the dead-zone and successfully retained control performance. The tracking error effectively decreases to less than 1% and there is not a chattering phenomenon in the air motor system.

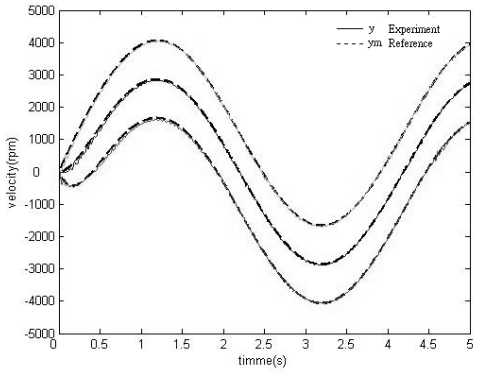

Fig. 12. MRAC with fuzzy friction $u_f = K_s \,\mathrm{sgn}(Cx)$ compensation (the frequency of referential sinusoidal wave is 0.25 Hz).

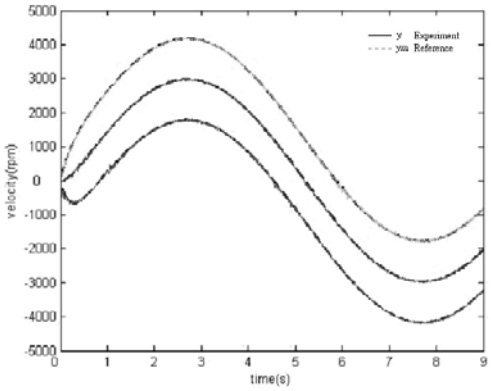

Fig. 13. MRAC with fuzzy friction $u_f = K_s \,\mathrm{sgn}(Cx)$ compensation (the frequency of referential sinusoidal wave is 0.1Hz).

7. Conclusion

In this research, we developed a model reference adaptive controller for a vane-type air motor. It was found that the reference signal's frequency plays an important role. For high frequency signals, the MRAC provides very good traction performance. However, for low frequency signals, the traction error

increases, the output starts chattering and a dead-zone sometimes appears due to the friction of the system. To improve the performance by compensating for the system's friction, we used fuzzy logic rules to modify the control input generated from the MRAC. The experimental results showed that the dead-zone disappears when the air motor is reversing its direction and the velocity is close to zero. Also, the tracking error decreased effectively and the system chattering disappeared.

References

[1] R. Richardson, M. Brown, B. Bhakta and M. Levesley, Impedance control for a pneumatic robot-based around pole-placement, joint space controllers,*Control. Eng. Pract.* 13 (3) (2005) 291-303.

[2] Y. Zhang and A. Nishi, Low-pressure air motor for wall-climbing robot actuation, *Mechatronics* 13 (4) (2003) 377-392.

[3] S.R. Pandian, F. Takemura,, Y. Hayakawaand S. Kawamura, Control performance of an air motor-can air motors replace electric motors?, *IEEE Int. Conf. on.*1 (1999) 518–524.

[4] M. O. Tokhi, M. Al-Miskiryand M. Brisland,Real-time control of air motors using a pneumatic H-bridge, *Control. Eng. Pract.*, 9 (4) (2001) 449-457.

[5] J. Pu, P.R. Moore and R. H. Weston, Digital servo motion control of air motors, *Int. J. Prod. Res.* 29 (3) (1991) 599-618.

[6] J. Wang, J. Puand P. R. Moore, Modelling study and servo-control of air motor systems, *Int. J. Control.* 71 (3) (1998) 459- 476.

[7] J. Wang, J. Pu, C. B. Wongand and P. R. Moore, Robust servo motion control of air motor systems, *UKACC Int Conf on Control.* 1 (1996) 90-95.

[8] X. S. Wang, H. Hongand C. Y. Su, Model reference adaptive control of continuous-time systems with an unknown input dead-zone, *IEE Proc.-Control Theory Appl.* 150 (3) (2003) 261 – 266.

[9] T. Senjyu, T. Kashiwagiand K. Uezato, Position control of ultrasonic motors using MRAC and dead-zone compensation with fuzzy inference, *IEEE Trans. Power Electron.* 17 (2) (2002) 265 – 272.

[10] T. Senjyu, T. Kashiwagiand K. Uezato, Position control of ultrasonic motors using MRAC with dead-zone compensation, *IEEE Trans. Power Electron.* 48 (6) (2001) 1278 – 1285.

[11] D. Zhou, T. L. Shen, K. Tamura, T. Nakazawa and N. Henmi, Adaptive control of a pneumatic valve with unknown parameters and disturbances, *SICE 2003 Ann. Conf.*3 (2003) 2703 – 2707.

[12] Y. R. Hwangand M. Tomizuka, Fuzzy smoothing algorithms for variable structure systems, *IEEE Trans. Fuzzy Syst.* 2 (4) (1994) 277-284.

[13] C.C. Lee, Fuzzy Logic in Control System: Fuzzy Logic Controller-Part I & II *IEEE Trans.Syst. Man. Cybern.* 20(2) 404-435.

[14] M. Mizumoto, Fuzzy reasoning and fuzzy control, Computrol. 28 (1989) 32-45.

[15] L. A Zadeh, Fuzzy Sets, *Inf. Control.* 8 (1965) 338-353.